



Research article

Low folate induces abnormal neuronal maturation and DNA hypomethylation of neuronal differentiation-related genes in cultured mouse neural stem and progenitor cells



Ryota Araki^{*}, Shoji Nishida, Yuki Nakajima, Arimi Iwakumo, Hayato Tachioka, Ayami Kita, Takeshi Yabe^{**}

Laboratory of Functional Biomolecules and Chemical Pharmacology, Faculty of Pharmaceutical Sciences, Setsunan University, 45-1 Nagaotoge-cho, Hirakata, Osaka 573-0101, Japan

ARTICLE INFO

Keywords:

Folate
Neuronal immaturity
Neural stem cells
DNA methylation
S-adenosylmethionine

ABSTRACT

Folate deficiency in a fetus is well known to cause neurodevelopment defects and development disorders. A low level of folate is also thought to be a risk for depression in adults. We have previously shown that post-weaning low folate induces neuronal immaturity in the dentate gyrus in mice, which suggests that low folate causes neuropsychological disorders via inhibition of neuronal maturation. In this study, we examined the effects of low folate on expression and epigenetic modification of genes involved in neuronal differentiation and maturation in primary mouse neural stem/progenitor cells (NSPCs) *in vitro*. An increase in Nestin (NSPC marker)-positive cells was observed in cells differentiated in a low folate medium for 3 days. An increase in β III-tubulin (Tuj1: immature neuron marker)-positive cells and a decrease in microtubule-associated protein 2 (MAP2: mature neuron marker)-positive cells were observed in cells differentiated in a low folate medium for 7 days. In these cells, mRNA levels for genes involved in neuronal differentiation and maturation were altered. Hypomethylation of DNA, but not of histone proteins, was also observed at some promoters of these neuronal genes. The level of S-adenosylmethionine (SAM), a methyl donor, was decreased in these cells. The abnormalities in neural maturation and changes in gene expression in culture under low folate conditions were partially normalized by addition of SAM (5 μ M). Based on these results, decreased SAM may induce DNA hypomethylation at genes involved in neuronal differentiation and maturation under low folate conditions, and this hypomethylation may be associated with low folate-induced neuronal immaturity.

1. Introduction

Neural stem/progenitor cells (NSPCs) are self-renewing and multipotent cells that can differentiate into cells such as neurons and glia [1]. To form the sophisticated mammalian central nervous system (CNS), maintenance and differentiation of NSPCs are strictly controlled by complex mechanisms, including epigenetic regulation [2, 3, 4, 5, 6]. Differentiation from NSPCs to neurons is most active in the embryonic brain and is required for brain development. This differentiation continues throughout life in specific brain regions, such as the subgranular zone (SGZ) of the dentate gyrus (DG) in the hippocampus. Newborn neurons from NSPCs in the SGZ are functionally integrated into existing neural circuits in the DG [1, 7], and are required for responses to stress

and antidepressant [8, 9]; therefore, abnormalities in newborn neurons are thought to be involved in neuropsychological disorders [10].

Folate is a B vitamin that serves as a source for transfer of one-carbon units in several biosynthetic reactions, including DNA and histone methylation [11]. Since these reactions play crucial roles in regulation of gene expression, folate deficiency induces biological dysfunction throughout the body, including the CNS. A low level of folate during pregnancy has been associated with fetal neural tube defects and developmental disorders such as autism spectrum disorders [12, 13]. Low folate can also lead to an increased risk of depression [14, 15, 16, 17, 18, 19, 20]. We have previously found an increase in immature neurons and a decrease in newborn mature neurons in the DG of mice fed a low folate diet. Furthermore, these mice show a depression-like state, such as

* Corresponding author.

** Corresponding author.

E-mail addresses: r-araki@pharm.setsunan.ac.jp (R. Araki), yabe@pharm.setsunan.ac.jp (T. Yabe).

increased immobility in the forced swim test [21]. These findings suggest that neuronal immaturity of newborn neurons may underlie psychiatric disorders such as depression; however, the mechanisms through which low folate levels cause neuronal immaturity are unclear.

In this study, to investigate these mechanisms, we examined epigenetic modifications such as DNA and histone methylation at genes involved in neuronal differentiation and maturation in cells differentiated from primary NSPCs in a low folate medium.

2. Material and methods

2.1. Cell culture

Primary NSPCs were prepared as previously reported with minor modifications [22]. Briefly, primary NSPCs were isolated from telencephalon of ddY outbred mice at E14.5 and cultured in Dulbecco's Modified Eagle's Medium (DMEM)/Ham's F-12 (Nacalai tesque, Kyoto, Japan) supplemented with 1% (v/v) N-2 supplement (Invitrogen, Carlsbad, CA, USA), 20 ng/ml epidermal growth factor (PeproTech, Rocky Hill, NJ, USA), 20 ng/ml fibroblast growth factor 2 (PeproTech) and 2 µg/ml heparin (Nacalai tesque) on non-treated 100 mm dishes. After 7 days in culture, neurospheres that formed were gathered and dissociated into a single cell suspension by pipetting. For differentiation of NSPCs, dissociated cells were plated on laminin/poly-L-ornithine-coated 24-well plates, 35-mm dishes or 100-mm dishes, and cultured in control (DMEM/Ham's F-12, folic acid 2.44 mg/l) or low folate (DMEM without

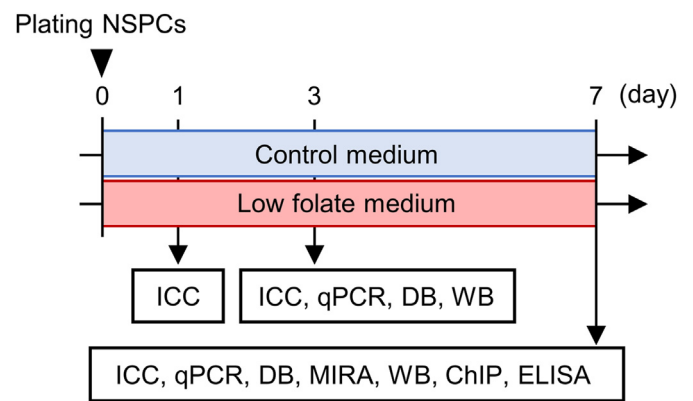


Figure 1. Schematic showing the experimental design. For differentiation, dissociated NSPCs were plated and cultured in control (folic acid 2.44 mg/l) or low folate (folic acid 0.66 mg/l) medium. Immunocytochemistry (ICC) was examined 1, 3 or 7 days after plating (differentiation days 1, 3 or 7). Quantitative RT-PCR (qPCR), dot blot (DB), and Western blot (WB) were performed on differentiation day 3 or 7. A methylated-CpG island recovery assay (MIRA), chromatin immunoprecipitation (ChIP) assay and an enzyme-linked immunosorbent assay (ELISA) were performed on differentiation day 7.

folic acid (Sigma-Aldrich, St. Louis, MO, USA):Ham's F-12 (Nacalai tesque) 1:1, folic acid 0.66 mg/l) medium supplemented with 2% (v/v) B-27 supplement (Invitrogen). For SAM supplementation experiments, SAM

Table 1. List of antibodies.

Immunochemistry					
Primary antibody					
Antigen	Dilution	Host	Source	Identifier	
Nestin	1:200	Mouse	Sigma-Aldrich, St. Louis, MO, USA	Cat#: MAB353; RRID: AB_94911	
Tuj1	1:1,000	Mouse	BioLegend, San Diego, CA, USA	Cat#: 801202; RRID: AB_10063408	
MAP2	1:1,000	Rabbit	Sigma-Aldrich, St. Louis, MO, USA	Cat#: AB5622; RRID: AB_91939	
GFAP	1:200	Rabbit	Agilent, Santa Clara, CA, USA	Cat#: Z0334; RRID: AB_10013382	
Secondary antibody					
Antigen	Dilution	Host	Conjugate	Source	Identifier
Mouse IgG	1:1,000	Donkey	Alexa Fluor 488	Thermo Fisher Scientific, Waltham, MA, USA	Cat#: A-11029; RRID: AB_138404
Rabbit IgG	1:1,000	Donkey	Alexa Fluor 488	Thermo Fisher Scientific, Waltham, MA, USA	Cat#: A-11008; RRID: AB_143165
Rabbit IgG	1:1,000	Donkey	Alexa Fluor 594	Thermo Fisher Scientific, Waltham, MA, USA	Cat#: A-21207; RRID: AB_141637
Dot blot					
Primary antibody					
Antigen	Dilution	Host	Source	Identifier	
5-Mehtylcytosine	1:2,000	Mouse	Active Motif, Carlsbad, CA, USA	Cat#: 61479; RRID: AB_2793653	
Secondary antibody					
Antigen	Dilution	Host	Conjugate	Source	Identifier
Mouse IgG	1:5,000	Horse	HRP	Cell Signaling Technology, Danvers, MA, USA	Cat#: 7076; RRID: AB_330924
Western blot					
Primary antibody					
Antigen	Dilution	Host	Source	Identifier	
Histone H3	1:1,000	Rabbit	Cell Signaling Technology, Danvers, MA, USA	Cat#: 9715; RRID: AB_331563	
Tri-methyl-histone H3 Lys4	1:1,000	Rabbit	Cell Signaling Technology, Danvers, MA, USA	Cat#: 9751; RRID: AB_2616028	
Tri-methyl-histone H3 Lys9	1:1,000	Rabbit	Cell Signaling Technology, Danvers, MA, USA	Cat#: 13969; RRID: AB_2798355	
Tri-methyl-histone H3 Lys27	1:1,000	Rabbit	Cell Signaling Technology, Danvers, MA, USA	Cat#: 9733; RRID: AB_2616029	
Tri-methyl-histone H3 Lys36	1:1,000	Rabbit	Cell Signaling Technology, Danvers, MA, USA	Cat#: 4909; RRID: AB_1950412	
Secondary antibody					
Antigen	Dilution	Host	Conjugate	Source	Identifier
Rabbit IgG	1:1,000	Goat	HRP	Cell Signaling Technology, Danvers, MA, USA	Cat#: 7074; RRID: AB_2099233
ChIP assay					
Antigen	Dilution	Host	Source	Identifier	
Tri-methyl-histone H3 Lys9	1:50	Rabbit	Cell Signaling Technology, Danvers, MA, USA	Cat#: 9751; RRID: AB_2616028	
Tri-methyl-histone H3 Lys27	1:50	Rabbit	Cell Signaling Technology, Danvers, MA, USA	Cat#: 9733; RRID: AB_2616029	

Table 2. List of primers.

Target gene	Forward primer (5' to 3')	Reverse primer (5' to 3')
Quantitative RT-PCR		
<i>Pax6</i>	GAGACTGGCTCCATCAGACC	CTAGCCAGGTTGCGAAGAAC
<i>Sox2</i>	ACCGTTTTTCGTGGTCTTGTT	CGATATCAACCTGCATGGAC
<i>Nrsf</i>	ACCTGCAGCAAGTGCAACTA	TTCACATTTATACGGGCGTTC
<i>Bmp4</i>	TGAGCCITTCAGCAAGTIT	CTTCCCGGTCTCAGGTATCA
<i>Stat3</i>	TGAAGGTGGTGGAGAACCTC	TTCTGCACGTACTCCATTGC
<i>Hey1</i>	GGTACCAGTGCCTTTGAGA	ATGCTCAGATAACGGGCAAC
<i>Ascl1</i>	AACAAACCAGACAGCCAACC	AGGAACCCATCTGTGATTGG
<i>Neurog1</i>	AGGACGAAGAGCAGGAACG	CAGGGCCAGATGTAGTTGT
<i>Eomes</i>	TGTGAGTGTAGGGTCTCTGA	CTCCTTCCTTCTCTCTCC
<i>Mef2c</i>	GGGGACTATGGGGAGAAAAA	ACAGCTTGTGGTGGTGTG
<i>Prox1</i>	CTTGACTCGGGACACAACAA	TGATTGGGTGATAGCCCTTC
<i>Neurod1</i>	GAGGCTCCAGGGTTATGAGA	GCTCTCGTGTATGATTGG
<i>Mib1</i>	CATTTCGATGGAAATGTGCAG	ACTCTGGCACCAGCAAAGAT
<i>Creb1</i>	GGAGCTTGTACCACCGTAA	GCAGATGATGTTGCATGAGC
<i>Gapdh</i>	ATGTTGAAGTTCGGTGTG	ACTCCACGACATACTCAG
Methylated-CpG island recovery assay		
<i>Pax6</i>	AGCACAGGACGAAAGAATGC	CGAAGGAAGCTCAAATCACACG
<i>Nrsf</i>	ACCGCGGTCTGAAACTTC	TTCCGGCCCTGCTACGAC
<i>Stat3</i>	CTAACCGGATCGCTGAGGTAC	CCGCTGGCCTCTCCTAG
<i>Hey1</i>	CAACCTCTCCGCTTCCC	CCGGTTAAAACCTCAACCATCCC
<i>Neurog1</i>	ACAGTAAGTGGCTTCGAAG	TCAGAGATGCAGGTCTCCAAG
<i>Eomes</i>	TTTCCCGTGTATCGCATTG	ATTACGGACGCCTGCAGTAG
<i>Mef2c</i>	AGCAAGGATGAAGTGGTACTG	AGTCGAGATCTTCTTCTGACC
<i>Prox1</i>	CTCTCCCAGCCCTCAC	GGTCCCAGCACCAATCG
<i>Neurod1</i>	GAAGACCATATGGCGCATGC	CATTCACCCCTCCCAGAAC
<i>Mib1</i>	CGAAAGGCTGCTCGTGGAC	CGGCGGGGAATCGTGAG
<i>Creb1</i>	AGTTTGACGCGGTGTGTTAC	TCTTACCGGTGTACAAGCTC
Chromatin immunoprecipitation assay		
<i>Pax6</i>	TTGCTGGCGTGGATATTAAGG	ATCTGACAACCGGGTCTACG
<i>Nrsf</i>	GGGAAGGGGGCGTGTCCG	CGCACATTCAGCACAGGA
<i>Stat3</i>	CGGGGCTTAGGAAGTACAGC	TACAGCCCTCCAGCCAATC
<i>Hey1</i>	CAACCTCTCCGCTTCCC	CCGGTTAAAACCTCAACCATCCC
<i>Neurog1</i>	GCCGTACTTAAGGGTCTCTG	GGCTGTCTCTGAGTGATG
<i>Eomes</i>	ATAGCAAAGTCCCTAGCCATG	TCTAGGCATACTGACCCGTTG
<i>Mef2c</i>	ACTAACAGTGTAGAGGCTTGGG	AACCAGACCTTTGTGAGTGC
<i>Prox1</i>	ACGTGCAGTCTTCTGTITTC	GCTTTCAGCGCTCTCTC
<i>Neurod1</i>	CGTCTCAGCATCAGCAACTC	TGACGATCTCATAACCCCTGGAG
<i>Mib1</i>	TTAGCGATCCGTTTCTTCCC	TCAGCGACACGGGATGG
<i>Creb1</i>	GGTGCAGCTCGGTGTITTC	CCGACTGAGGAGCCGACG

(New England Biolabs, Ipswich, MA, USA) was added to a control or a low-folate medium at a final concentration of 5 μ M at the planting of NSPCs. Thereafter, the same amount of SAM was added every 24 h. Immunocytochemistry was examined at differentiation days 1, 3 or 7 after plating of NSPCs. Quantitative RT-PCR, dot blot, Western blot, methylated-CpG island recovery, chromatin immunoprecipitation (ChIP) assay, and enzyme-linked immunosorbent assay (ELISA) for SAM were performed on day 7. A schematic of the experimental design is shown in Figure 1.

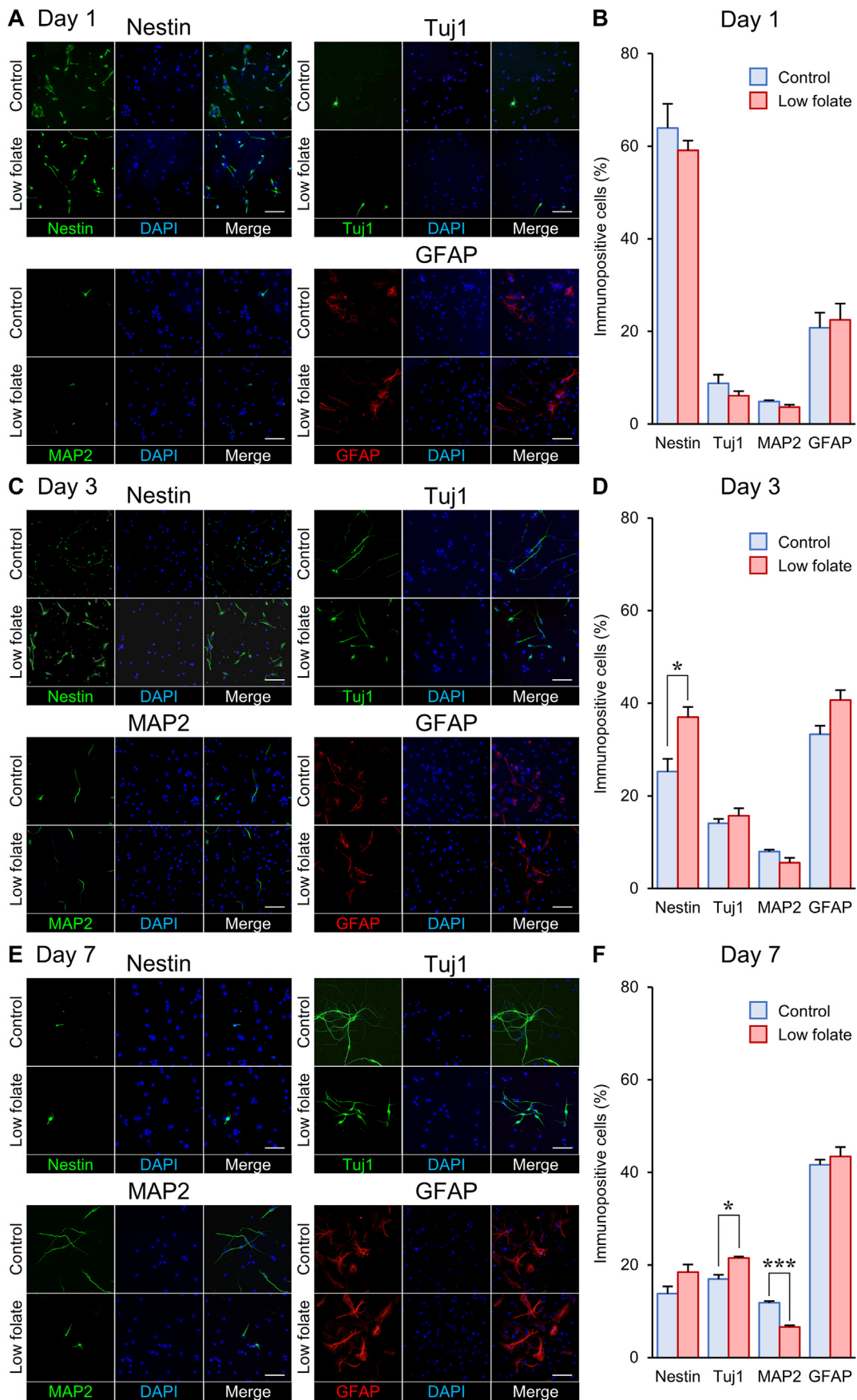
2.2. Immunocytochemistry

Immunocytochemistry was performed as previously reported with minor modifications [22]. Briefly, differentiated NSPCs were fixed with 4% paraformaldehyde at room temperature for 30 min and with 80% methanol at -20 $^{\circ}$ C for 20 min. To block nonspecific antibody binding, fixed cells were incubated with 1% BSA in Tris-buffered saline with 0.3% Triton X-100 (PBS-T) at 4 $^{\circ}$ C for 2 h. Then, cells were incubated at 4 $^{\circ}$ C overnight with a primary antibody, followed by incubation at room

temperature for 1 h with a secondary antibody. The primary and secondary antibodies (Table 1) were diluted with 1% BSA in PBS-T. Nuclear counterstaining was performed with DAPI. Images were collected using microscope (BX53; Olympus, Tokyo, Japan) with CCD camera (DP73; Olympus). Five visual fields (0.36 mm²; average number of cells per field of view 40) were captured randomly for each well, and data were obtained by averaging the results of the five fields of view. All images were captured under the same excitation intensity and exposure time. The number of cells immunopositive for Nestin, Tuj1, MAP2, or GFAP was determined relative to the number of DAPI-stained nuclei. The percentage of positive cells was determined out of the total number of counted cells stained by DAPI. The numbers of immunopositive cells were measured by an observer blinded to the treatment conditions.

2.3. Quantitative RT-PCR

Total RNA was isolated from differentiated NSPCs with Sepasol-RNA I Super G (Nacalai tesque) and used (1 μ g) in reverse transcription with ReverTra Ace (Toyobo, Osaka, Japan). Quantitative PCR was performed



(caption on next page)

Figure 2. Effects of low folate on neuronal differentiation of NSPCs on differentiation days 1 (A,B), 3 (C,D) and 7 (E,F). Representative photomicrographs of Nestin- (green), Tuj1- (green), MAP2- (green), and GFAP- (red) positive cells were shown (A,C,E). The number of Nestin-positive cells increased on differentiation day 3, but decreased on differentiation day 7 under low folate conditions. The number of Tuj1-positive cells increased and the number of MAP2-positive cells decreased on differentiation day 7, but not on days 1 and 3, under low folate conditions. The number of GFAP-positive cells did not differ between control and low folate conditions (B,D,F). Five visual fields (0.36 mm²) were captured randomly for each well, and data were obtained by averaging the results of the five fields of view. The numbers of the markers-immunopositive cells and DAPI-stained cells were shown in Table 3. The number of cells immunopositive for Nestin, Tuj1, MAP2, or GFAP was determined relative to the number of DAPI-stained nuclei. The percentage of positive cells was determined out of the total number of counted cells stained by DAPI. Values are shown as the mean \pm SEM of 3 wells. * $P < 0.05$, *** $P < 0.001$. Scale bar = 30 μ m.

with Thunderbird qPCR Mix (Toyobo) and primers (Table 2, using Thermal Cycler Dice Real Time System Single (Takara Bio, Shiga, Japan). Expression levels of genes were normalized against the endogenous *Gapdh* standard. Relative gene expression was calculated using the $\Delta\Delta C_T$ method.

2.4. Dot blot

Genomic DNA was extracted from differentiated NSPCs with DNA extraction buffer (150 mM NaCl, 10 mM Tris-HCl; pH 8.0, 10 mM EDTA, 0.1% SDS and 100 μ g/ml proteinase K), and isolated with Phenol Saturated with TE buffer, phenol:chloroform:isoamyl alcohol 25:24:1 (pH 7.9) (both Nacalai tesque), and ethanol. Isolated DNA was measured by BioSpec-nano (Shimadzu, Kyoto, Japan) for concentration, diluted to 10 ng/100 μ l in 0.4 mM NaOH/10 mM EDTA, denatured at 99 °C for 10 min, and then placed on ice immediately. The denatured DNA solution (10 ng DNA) was neutralized with 100 μ l of 2 M ammonium acetate and spotted onto a nitrocellulose membrane (Bio-Rad, Hercules, CA, USA) using a dot-blotter (Sanplatec, Osaka, Japan). After rinsing with 2 \times SSC and complete drying, spotted DNA was fixed with UV irradiation (302 nm) using 2UV Transilluminator (UVP, Upland, CA, USA). The membrane was then blocked with Blocking one solution (Nacalai tesque) and incubated with a primary antibody to 5-methylcytosine at 4 °C overnight, followed by incubation with a secondary antibody at room temperature for 1 h. The primary and secondary antibodies (Table 1) were diluted with 5% Blocking one solution in Tris-buffered saline with 0.05% Tween-20 (TBS-T). The dot signal was detected with Chemi-Lumi One L (Nacalai tesque) using ChemiDoc MP (Bio-Rad). The fold changes for methylation levels were calculated as a ratio to the mean of controls.

2.5. Methylated-CpG island recovery assay

Genomic DNA of differentiated NSPCs was isolated using DNA extraction buffer (150 mM NaCl, 10 mM Tris-HCl; pH 8.0, 10 mM EDTA, 0.1% SDS and 100 μ g/ml proteinase K). To shear the DNA, the isolated genomic DNA was sonicated for 5 s with Handy sonic (UR-21P; Tomy Seiko, Tokyo, Japan) and purified with phenol:chloroform:isoamyl alcohol 25:24:1 (pH 7.9) (Nacalai tesque) and ethanol. The sheared DNA (1 μ g) was used for enrichment of methylated DNA with EpiXplore Methylated DNA Enrichment Kit (Takara Bio). Quantitative real-time PCR was performed with KOD qPCR Mix (Toyobo) and primers (Table 2), using Thermal Cycler Dice Real Time System Single (Takara Bio). DNA methylation levels were calculated as methylated DNA/total DNA. The fold changes for methylation levels were calculated as a ratio to the mean of controls.

2.6. Histone extraction and Western blot

Histone extraction was performed as previously reported with minor modifications [23]. Differentiated NSPCs were harvested with 1 ml of homogenization buffer (50 mM Tris-HCl; pH 7.5, 25 mM KCl, 250 mM sucrose, 2 mM sodium butyrate, 0.5 mM phenylmethylsulphonyl fluoride (PMSF), protease inhibitor cocktail). The harvested cells were homogenized with 12 strokes in a pre-cooled Dounce tissue grinder with a tight pestle (Wheaton, Millville, NJ, USA). The homogenate was centrifuged at 7,700 \times g for 1 min at 4 °C, and the supernatant (cytoplasmic fraction) was removed. The pellet (nuclear fraction) was suspended in 500 μ l of 0.4

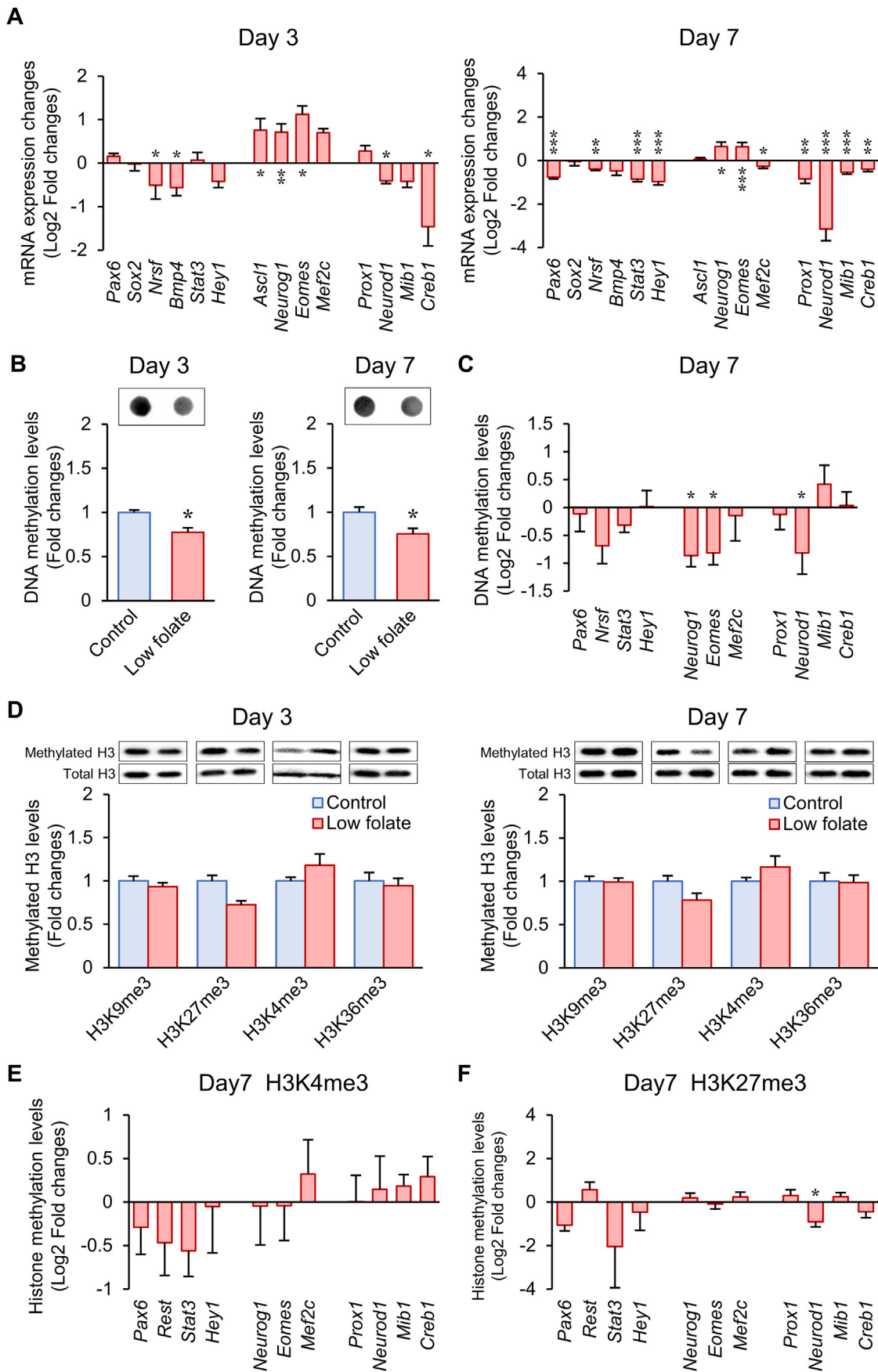
N H₂SO₄ and incubated for 30 min on ice to extract histones. The suspension was centrifuged at 15,000 \times g for 10 min at 4 °C. The supernatant was mixed with 250 μ l of 100% trichloroacetic acid containing 10 mM deoxycholic acid, incubated for 30 min on ice, and centrifuged at 15,000 \times g for 5 min at 4 °C. The precipitated proteins were washed with 1 ml of acidified acetone (0.1% HCl) for 5 min and 1 mL of pure acetone for 5 min. The purified protein pellets were resuspended in 10 mM Tris-HCl (pH 8.0) and protein concentrations were determined using BCA Protein Assay Kit (Thermo Fisher Scientific). Protein samples were boiled for 10 min in sample buffer (0.1 M Tris-HCl (pH 6.8), 2% SDS, 4.2% 2-mercaptoethanol, 10% glycerol and 0.005% bromophenol blue). Aliquots (200 ng protein) were subjected to SDS-PAGE in 15% polyacrylamide gels and transferred to a PVDF membrane (Millipore, Burlington, MA, USA). The membranes were blocked with 3% skim milk (Nacalai tesque) in TBS-T at room temperature for 1 h and incubated at 4 °C overnight with a primary antibody (Table 1), followed by incubation at room temperature for 1 h with a secondary antibody (Table 1). The signal was detected with Chemi-Lumi One L (Nacalai Tesque) using ChemiDoc MP. The methylation levels of histone H3 were calculated relative to the total histone H3 level. The fold changes for methylation levels were calculated as a ratio to the mean of controls.

2.7. ChIP assay

The ChIP assay was performed as previously reported with minor modifications [24]. Briefly, for crosslinking of histone-DNA complexes, differentiated NSPCs were fixed with DMEM/Ham's F-12 containing 1% formaldehyde at room temperature for 10 min. To stop the crosslinking reaction, 5 ml of glycine solution from ChIP-IT Express Kit (Active Motif, Carlsbad, CA, USA) was added to the fixed cells. The cells were incubated at room temperature for 5 min and harvested with 1 ml of supplied Cell scraping solution containing 0.5 mM PMSF. The cell solution was then centrifuged at 800 \times g for 10 min at 4 °C. The cell pellet was suspended in 500 μ l of supplied Lysis buffer containing protease inhibitor cocktail and 0.5 mM PMSF, and the solution was incubated for 30 min on ice. For release of nuclei, the cell solution was homogenized with 12 strokes in a pre-cooled Dounce tissue grinder (Wheaton) with a tight pestle. The homogenate was centrifuged at 2,400 \times g for 10 min at 4 °C. After removing supernatant, the nuclei pellet was resuspended in 150 μ l of supplied Shearing buffer. To shear the chromatin, the nuclei solution was sonicated 10 times for 30 s with Handy sonic (UR-21P; Tomy Seiko). The sheared chromatin solution was centrifuged at 18,000 \times g for 10 min at 4 °C and ChIP procedures was performed using the ChIP-IT Express Kit. Immunoprecipitation was performed using anti-trimethylhistone antibodies (Table 1) on a rotator overnight at 4 °C. ChIP DNA and Input DNA were purified with phenol:chloroform:isoamyl alcohol 25:24:1 (pH 7.9) (Nacalai tesque) and ethanol. Quantitative real-time PCR was performed with KOD qPCR Mix (Toyobo) and primers (Table 2), using Thermal Cycler Dice Real Time System Single (Takara Bio). Histone methylation levels were calculated as ChIP sample/input sample. The fold changes for methylation levels were calculated as a ratio to the mean of controls.

2.8. ELISA

ELISA for SAM was performed using Mouse S-Adenosylmethionine ELISA kit (MyBioSource, San Diego, CA, USA). Cells were homogenized with RIPA buffer (Nacalai Tesque) and centrifuged at 10,000 \times g for 10



(caption on next page)

Figure 3. Gene expression and epigenetic modifications of genes encoding transcription factors involved in neuronal differentiation and maturation under low folate conditions. The mRNA levels for genes involved in maintenance or proliferation of NSPCs, such as *Pax6*, *Sox2*, *Nrsf*, *Bmp4*, *Stat3* and *Hey1*, or in neuronal maturation, such as *Prox1*, *Neurod1*, *Mib1* and *Creb1*, were downregulated with low folate on differentiation day 3 or 7. In contrast, mRNA levels for genes involved in neuronal differentiation, such as *Ascl1*, *Neurog1* and *Eomes*, were upregulated on differentiation day 3 or 7 (A). The 5-methylcytosine detected by dot blot analysis (shown in the photograph above each column; 10 ng DNA were spotted in each) on differentiation day 3 or 7 (B) and DNA methylation levels in CpG islands at promoters of *Neurog1* and *Eomes* on differentiation day 7 (C) were significantly decreased with low folate. H3K4me3, H3K9me3, H3K27me3 or H3K36me3 levels in the global genome were unchanged with low folate on differentiation day 3 or 7 (D). H3K4me3 (E) and H3K27me3 (F) in promoter regions were also unchanged except for *Neurod1* on differentiation day 7. Values are shown as the mean \pm SEM of 6 (A), 3 (B), 9 (C), 6 (D), and 9 cultures (E,F). The fold changes were calculated as a ratio to the mean of controls. For Figures A,C,E,F, the values of low folate group are shown on log scales. * $P < 0.05$, ** $P < 0.01$, *** $P < 0.001$ vs. control.

min at 4 °C. The supernatant was used for ELISA. The intracellular SAM levels were normalized against the total amount of protein.

2.9. Statistical analysis

All data are expressed as a mean \pm standard error of the mean (SEM). Data for Figures 2, 3 and 4A were analyzed by Student *t*-test. Data in Figures 4B, 5B, 5D, 5F, 5H, 6B, 6D, 6F and 6H were analyzed using one- (Figure 4B) and two-way analysis of variance (ANOVA) (Figures 5B, 5D, 5F, 5H, 6B, 6D, 6F, 6H) followed by a Tukey-Kramer *post-hoc* test. All analyses were performed using Statview 5.0J for Apple Macintosh (SAS Institute Inc., Cary, NC, USA). A value of $p < 0.05$ was considered to be significant.

3. Results

3.1. Low folate causes neuronal immaturity in primary NSPCs

To investigate the mechanisms of low folate-induced neuronal immaturity, murine embryonic telencephalon-derived NSPCs, which

have a high potential to differentiate into neurons, were differentiated in a low folate medium. Immunofluorescence analyses showed an increase in Nestin (NSPC marker)-positive cells on day 3 of differentiation, and an increase in β III-tubulin (Tuj1: immature neuron marker)-positive cells and a decrease in microtubule-associated protein 2 (MAP2: mature neuron marker)-positive cells on day 7 of differentiation. On day 1, there was no difference in the number of each type of positive cells between the control and low folate conditions, and there was no difference in the number of glial fibrillary acidic protein (GFAP: astrocyte marker)-positive cells in control and low folate conditions over days 1–7 (Figure 2A,B,C,D,E,F). Thus, as found in the DG of folate deficient mice [21], low folate-induced neuronal immaturity was observed in cultured NSPCs.

3.2. Low folate alters expression and epigenetic modifications in genes involved in neuronal differentiation and maturation

Next, we examined expression patterns of genes involved in neuronal differentiation and maturation. Under low folate conditions, mRNA levels for genes encoding transcription factors involved in maintenance

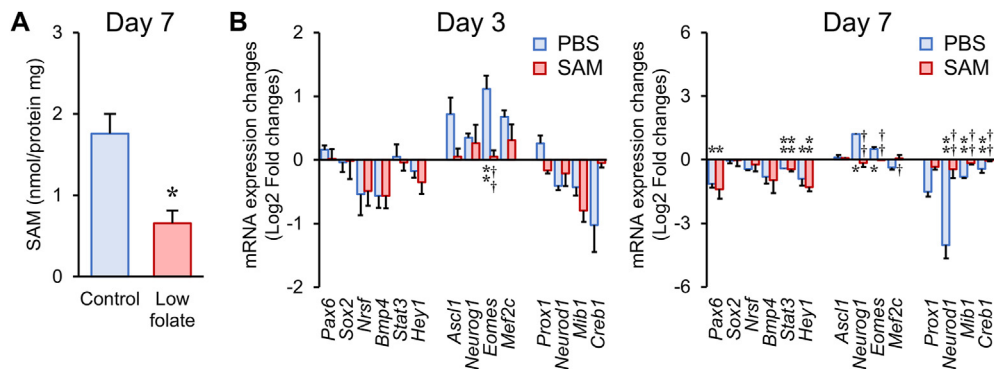


Figure 4. Effects of SAM supplementation (5 μ M) on abnormalities in mRNA expression in cells differentiated from NSPCs in a low folate medium. On differentiation day 7, intracellular SAM was significantly decreased in cells differentiated from NSPCs in low folate (A). Changes of mRNA expression for genes involved in neuronal differentiation and maturation (B) were reversed by supplementation of SAM. Values are shown as the mean \pm SEM of 3. For Figure B, the values of low folate with/without SAM group are shown on log scales. * $P < 0.05$, ** $P < 0.01$ vs. control with PBS, $^{\dagger}P < 0.05$, $^{\ddagger}P < 0.01$ vs. low folate with PBS. The results of one-way ANOVA for Day3 in Figure B: $F_{(2,6)} = 0.65$, $P > 0.05$ for *Pax6*; $F_{(2,6)} < 0.01$, $P > 0.05$ for *Sox2*; $F_{(2,6)} = 1.14$, $P > 0.05$ for *Nrsf*; $F_{(2,6)} = 4.23$, $P > 0.05$ for *Bmp4*; $F_{(2,6)} = 0.09$, $P > 0.05$ for *Stat3*; $F_{(2,6)} = 2.14$, $P > 0.05$ for *Hey1*; $F_{(2,6)} = 5.43$, $P < 0.05$ for *Ascl1*; $F_{(2,6)} = 0.85$, $P > 0.05$ for *Neurog1*; $F_{(2,6)} = 23.72$, $P < 0.01$ for *Eomes*; $F_{(2,6)} = 3.61$, $P > 0.05$ for *Mef2c*; $F_{(2,6)} = 3.16$, $P > 0.05$ for *Prox1*; $F_{(2,6)} = 2.54$, $P > 0.05$ for *Neurod1*; $F_{(2,6)} = 6.05$, $P < 0.05$ for *Mib1*; $F_{(2,6)} = 4.73$, $P > 0.05$ for *Creb1*. Day7: $F_{(2,6)} = 9.17$, $P < 0.05$ for *Pax6*; $F_{(2,6)} < 0.01$, $P > 0.05$ for *Sox2*; $F_{(2,6)} = 0.88$, $P > 0.05$ for *Nrsf*; $F_{(2,6)} = 1.44$, $P > 0.05$ for *Bmp4*; $F_{(2,6)} = 25.09$, $P < 0.01$ for *Stat3*; $F_{(2,6)} = 11.38$, $P < 0.01$ for *Hey1*; $F_{(2,6)} = 0.53$, $P > 0.05$ for *Ascl1*; $F_{(2,6)} = 19.97$, $P < 0.01$ for *Neurog1*; $F_{(2,6)} = 15.39$, $P < 0.01$ for *Eomes*; $F_{(2,6)} = 4.81$, $P < 0.05$ for *Mef2c*; $F_{(2,6)} = 32.81$, $P < 0.001$ for *Prox1*; $F_{(2,6)} = 22.09$, $P < 0.01$ for *Neurod1*; $F_{(2,6)} = 38.37$, $P < 0.001$ for *Mib1*; $F_{(2,6)} = 2.48$, $P > 0.05$ for *Creb1*.

Table 3. Number of cells/visual field (Mean \pm SEM).

Figure 2A		
Day 1		
	Number of DAPI-stained cells	Number of Nestin-immunopositive cells
Control	81.7 \pm 14.4	51.5 \pm 7.6
Low folate	107.0 \pm 5.0	61.8 \pm 0.8
	Number of DAPI-stained cells	Number of Tuj1-immunopositive cells
Control	98.0 \pm 5.6	8.0 \pm 0.8
Low folate	88.4 \pm 3.8	5.6 \pm 0.8
	Number of DAPI-stained cells	Number of MAP2-immunopositive cells
Control	95.3 \pm 3.1	4.8 \pm 0.8
Low folate	69.6 \pm 3.7	4.9 \pm 0.7
	Number of DAPI-stained cells	Number of GFAP-immunopositive cells
Control	76.5 \pm 17.2	23.0 \pm 4.2
Low folate	109.3 \pm 9.3	32.1 \pm 5.8
Figure 2B		
Day 3		
	Number of DAPI-stained cells	Number of Nestin-immunopositive cells
Control	76.0 \pm 3.4	18.6 \pm 1.7
Low folate	50.9 \pm 2.7	18.9 \pm 1.9
	Number of DAPI-stained cells	Number of Tuj1-immunopositive cells
Control	89.2 \pm 22.0	10.8 \pm 1.0
Low folate	80.0 \pm 8.4	12.8 \pm 2.2
	Number of DAPI-stained cells	Number of MAP2-immunopositive cells
Control	156.3 \pm 11.2	12.4 \pm 0.9
Low folate	113.3 \pm 3.7	6.1 \pm 1.1
	Number of DAPI-stained cells	Number of GFAP-immunopositive cells
Control	89.2 \pm 22.0	28.8 \pm 7.6
Low folate	80.0 \pm 8.4	33.6 \pm 5.6
Figure 2C		
Day 7		
	Number of DAPI-stained cells	Number of Nestin-immunopositive cells
Control	85.0 \pm 3.8	12.0 \pm 1.6
Low folate	69.4 \pm 5.0	12.6 \pm 1.8
	Number of DAPI-stained cells	Number of Tuj1-immunopositive cells
Control	123.4 \pm 8.1	20.2 \pm 1.4
Low folate	92.2 \pm 6.2	19.2 \pm 1.4
	Number of DAPI-stained cells	Number of MAP2-immunopositive cells
Control	89.2 \pm 2.5	10.1 \pm 0.3
Low folate	104.5 \pm 1.0	6.3 \pm 0.7
	Number of DAPI-stained cells	Number of GFAP-immunopositive cells
Control	123.4 \pm 8.1	50.4 \pm 3.0
Low folate	92.2 \pm 6.2	39.0 \pm 2.2
Figure 4C		
Day 3		
	Number of DAPI-stained cells	Number of Nestin-immunopositive cells
Control/PBS	93.8 \pm 9.2	17.6 \pm 1.2
Control/SAM	76.1 \pm 3.3	15.3 \pm 1.4
Low folate/PBS	103.2 \pm 5.0	50.8 \pm 4.0
Low folate/SAM	79.5 \pm 4.1	24.5 \pm 2.0

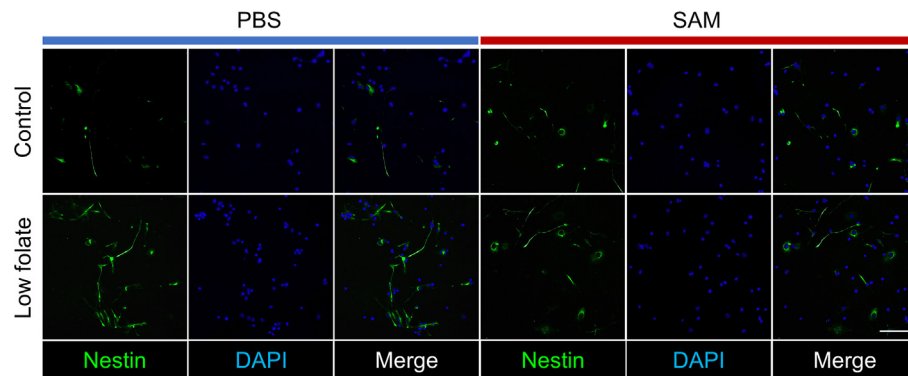
Table 3 (continued)

Tuj1	Number of DAPI-stained cells	Number of Tuj1-immunopositive cells
Control/PBS	61.7 \pm 4.1	10.1 \pm 0.7
Control/SAM	67.6 \pm 2.4	12.2 \pm 0.6
Low folate/PBS	92.2 \pm 6.2	19.2 \pm 1.4
Low folate/SAM	81.9 \pm 7.5	15.3 \pm 2.1
	Number of DAPI-stained cells	Number of MAP2-immunopositive cells
Control/PBS	74.7 \pm 3.9	4.9 \pm 1.3
Control/SAM	63.7 \pm 4.5	2.3 \pm 0.7
Low folate/PBS	81.7 \pm 5.2	4.3 \pm 0.4
Low folate/SAM	72.3 \pm 3.0	3.6 \pm 0.0
	Number of DAPI-stained cells	Number of GFAP-immunopositive cells
Control/PBS	85.0 \pm 3.2	31.4 \pm 2.2
Control/SAM	82.3 \pm 12.8	31.0 \pm 11.8
Low folate/PBS	90 \pm 5.8	39.6 \pm 3.9
Low folate/SAM	82.3 \pm 7.5	33.8 \pm 5.0
Figure 4D		
Day 7		
	Number of DAPI-stained cells	Number of Nestin-immunopositive cells
Control/PBS	83.6 \pm 6.8	2.0 \pm 1.0
Control/SAM	78.8 \pm 2.8	9.2 \pm 2.4
Low folate/PBS	86.4 \pm 3.4	10.8 \pm 1.4
Low folate/SAM	71.4 \pm 4.8	8.0 \pm 1.2
	Number of DAPI-stained cells	Number of Tuj1-immunopositive cells
Control/PBS	68.5 \pm 2.5	20.3 \pm 2.3
Control/SAM	60.5 \pm 7.5	28.0 \pm 6.5
Low folate/PBS	50.4 \pm 3.0	21.4 \pm 1.2
Low folate/SAM	67.0 \pm 3.5	22.0 \pm 5.0
	Number of DAPI-stained cells	Number of MAP2-immunopositive cells
Control/PBS	89.1 \pm 19.5	10.1 \pm 0.3
Control/SAM	81.1 \pm 3.8	8.9 \pm 0.5
Low folate/PBS	104.5 \pm 1.0	7.3 \pm 0.7
Low folate/SAM	97.2 \pm 6.6	11.0 \pm 2.5
	Number of DAPI-stained cells	Number of GFAP-immunopositive cells
Control/PBS	97.5 \pm 7.8	41.5 \pm 1.3
Control/SAM	98.4 \pm 10.0	43.8 \pm 4.7
Low folate/PBS	117.3 \pm 11.7	43.0 \pm 11.9
Low folate/SAM	105.7 \pm 5.8	43.0 \pm 5.7

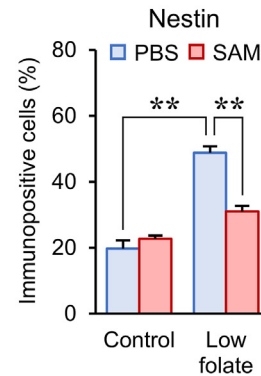
and proliferation of NSPCs such as *Pax6*, *Nrsf*, *Bmp4*, *Stat3* and *Hey*, and for genes involved in neuronal maturation such as *Prox1*, *Neurod1*, *Mib1* and *Creb1* were downregulated on differentiation day 3 or 7, compared with levels under control conditions. In contrast, mRNA levels for genes involved in neuronal differentiation such as *Ascl1*, *Neurog1* and *Eomes* were upregulated under low folate conditions (Figure 3A).

The molecular basis of the low folate-induced changes in neuronal gene expression was examined by analysis of DNA and histone methylation, which are epigenetic mechanisms in which folate-mediated one-carbon metabolism plays a critical role. DNA methylation commonly occurs at cytosines within 5'-CpG-3' dinucleotides. Sequences with a higher frequency of CpG dinucleotides than the rest of the genome are referred to as CpG islands and are often located in promoter and regulatory regions

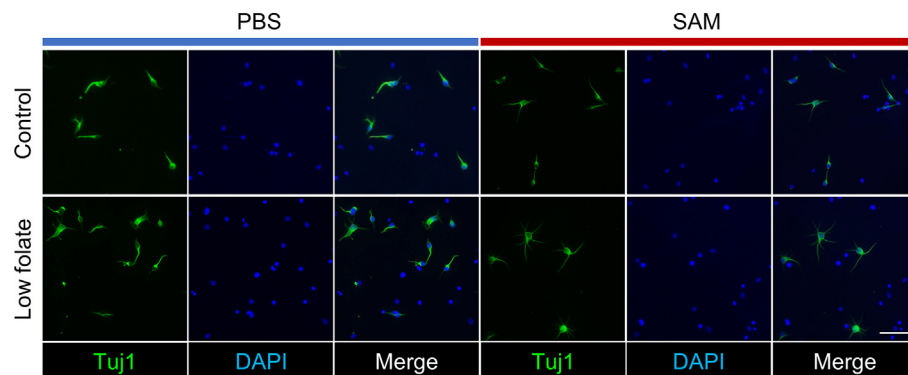
A Day 3 Nestin



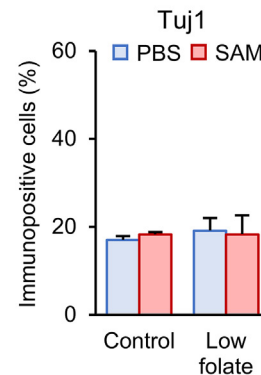
B Day 3



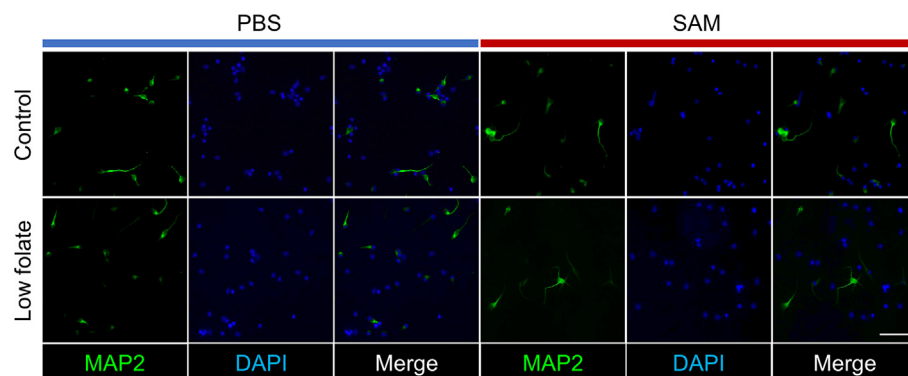
C Day 3 Tuj1



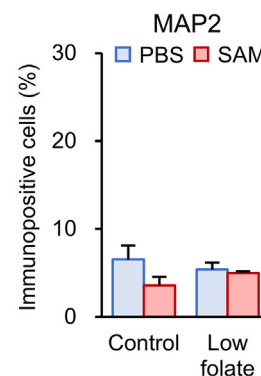
D Day 3



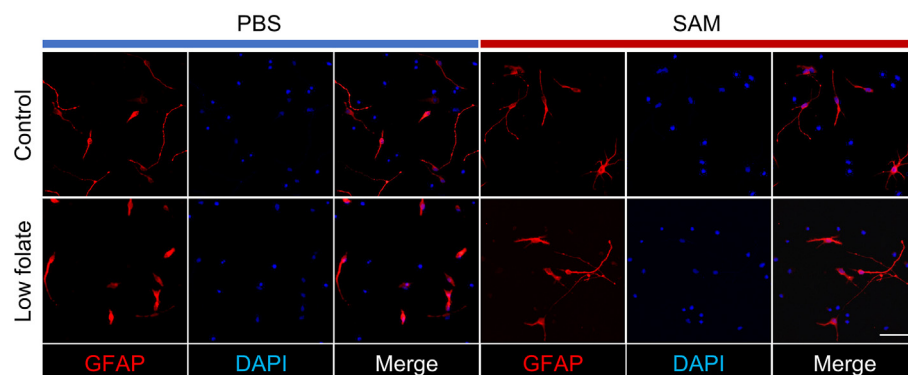
E Day 3 MAP2



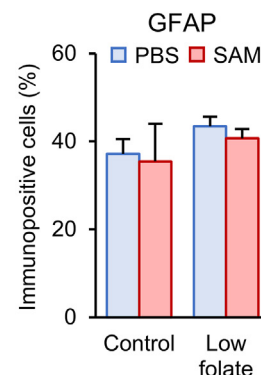
F Day 3



G Day 3 GFAP



H Day 3



(caption on next page)

Figure 5. Effects of SAM supplementation (5 μ M) on abnormalities in neuronal maturation in cells differentiated from NSPCs in a low folate medium on differentiation day 3. Representative photomicrographs of Nestin- (green) (A), Tuj1- (green) (C), MAP2- (green) (E), and GFAP- (red) positive cells (G) were shown. The increased number of Nestin-positive cells by a low folate medium was reversed by supplementation of SAM. SAM supplementation did not change the numbers of Tuj1-, MAP2- or GFAP-positive cells (B,D,F,H). Five visual fields (0.36 mm²) were captured randomly for each well, and data were obtained by averaging the results of the five fields of view. The numbers of the markers-immunopositive cells and DAPI-stained cells were shown in Table 3. The number of cells immunopositive for Nestin, Tuj1, MAP2, or GFAP was determined relative to the number of DAPI-stained nuclei. The percentage of positive cells was determined out of the total number of counted cells stained by DAPI. Values are shown as the mean \pm SEM of 3 cultures. The fold changes were calculated as a ratio to the mean of controls. ** $P < 0.01$. Scale bar = 30 μ m. Two-way ANOVA for revealed a main significant effect of folate ($F_{(1,8)} = 68.21, P < 0.001$) and SAM ($F_{(1,8)} = 13.11, P < 0.01$), and a significant interaction between folate and SAM ($F_{(1,8)} = 16.77, P < 0.01$) for Nestin; no significant effect of folate ($F_{(1,8)} = 0.16, P > 0.05$) or SAM ($F_{(1,8)} = 0.17, P > 0.05$) and no significant interaction between folate and SAM ($F_{(1,8)} = 0.08, P > 0.05$) for Tuj1; no significant effect of folate ($F_{(1,8)} = 2.81, P > 0.05$) or SAM ($F_{(1,8)} = 0.02, P > 0.05$) and no significant interaction between folate and SAM ($F_{(1,8)} = 1.60, P > 0.05$) for MAP2; and no significant effect of folate ($F_{(1,8)} = 0.21, P > 0.05$) or SAM ($F_{(1,8)} = 1.41, P > 0.05$) and no significant interaction between folate and SAM ($F_{(1,8)} = 0.01, P > 0.05$) for GFAP.

[25, 26]. Histone methylation involves lysine or arginine residues of histone H3 or H4 subunits. Histone H3 lysine methylation is relatively well understood with respect to gene expression and is implicated in both transcriptional activation and repression, depending on the methylation site. In particular, trimethylations of lysines 4 and 27 of histone H3 (H3K4me3 and H3K27me3) in promoter regions are regarded as activation and repression markers, respectively [27].

With this background, we examined DNA methylation and histone H3 trimethylation under low folate conditions. DNA methylation in the global genome was decreased in low folate conditions on differentiation days 3 and 7 (Figure 3B). DNA methylation in CpG islands at promoters of genes involved in neuronal differentiation and maturation such as *Neurog1*, *Eomes* and *Neurod1* was decreased in low folate conditions on differentiation day 7 (Figure 3C). In contrast to DNA methylation, there were no significant changes in H3K4me3, H3K9me3, H3K27me3 or H3K36me3 in the global genome between control and low folate conditions on differentiation days 3 and 7 (Figure 3D). The levels of H3K4me3 and H3K27me3 in genomic regions proximal to promoters of the evaluated genes were also unchanged with low folate, except for *Neurod1*, on differentiation day 7 (Figure 3E,F).

3.3. Low folate decreases intracellular S-adenosylmethionine in primary NSPCs

DNA methylation is mediated via transfer of a methyl group from S-adenosylmethionine (SAM) to DNA [28]. SAM is converted to S-adenosylhomocysteine (SAH) in this methylation reaction, and SAH is recycled back to SAM via homocysteine and methionine in the cytosol of cells. Folate is an important agent in conversion of homocysteine to methionine, which suggests that there may be low levels of intracellular SAM under low folate conditions. Thus, we examined intracellular SAM levels in cells differentiated from primary NSPCs, and found that SAM was lower with low folate compared to control conditions (Figure 4A). We next examined whether supplementation of SAM in a low folate medium could rescue abnormalities in neural maturation. Supplementation of SAM (5 μ M) in a low folate medium reversed the increased expression of genes involved in neuronal differentiation, such as *Neurog1* and *Eomes*, and the decreased expression of genes involved in neuronal maturation, such as *Prox1*, *Neurod1* and *Mib1*, on differentiation days 3 and 7. In contrast, SAM supplementation did not reverse the decreased expression of genes involved in maintenance and proliferation of NSPCs, such as *Pax6*, *Stat3* and *Hey1* (Figure 4B).

Similarly to expression of genes involved in neuronal differentiation and maturation, the increased number of Nestin-positive cells on differentiation day 3 (Figure 5A,B,C,D,E,F,G,H), and the increased number of Tuj1-positive cells and the decreased number of MAP2-positive cells on differentiation day 7 (Figure 6A,B,C,D,E,F,G,H) were reversed by SAM supplementation. SAM did not affect the number of GFAP-positive cells.

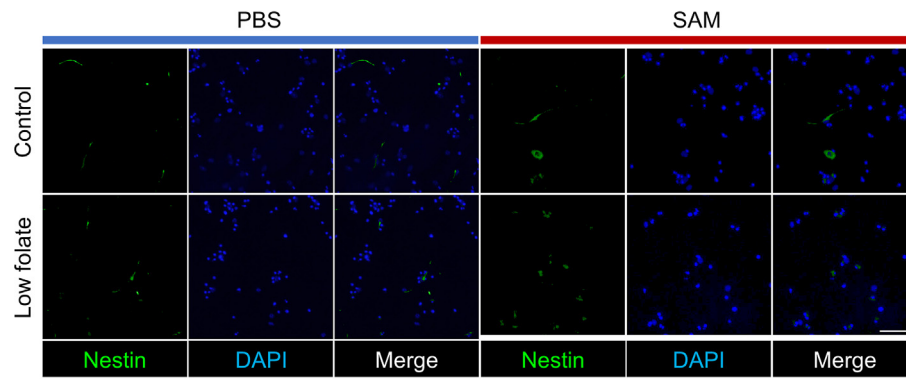
4. Discussion

There have been many studies of the effects of folate deficiency on proliferation, survival, differentiation and maturation of NSPCs *in vitro* and *in vivo* [29, 30, 31, 32, 33]. However, all of these studies have used

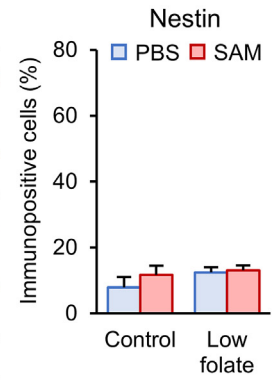
complete depletion of folate in the medium or in the diet. Under these conditions, the proliferation, survival and differentiation of NSPCs have been found to be markedly reduced. In contrast, in this study, we assessed the differentiation and maturation of NSPCs using a medium in which folate was reduced, but not completely removed, to mimic the neuronal immaturity that we have previously shown in the DG of mice fed a low folate, but not completely folate-deficient, diet [21]. Under the conditions used in this study, an increased number of immature neurons and a decreased number of mature neurons were observed in cells differentiated from NSPCs, as we previously reported in the DG [21]. The projections observed in Tuj1-positive cells and MAP2-positive cells on Day 7 appeared to be extremely short at low folate compared with controls. There were no differences between control and low folate conditions in the number of GFAP-positive astrocytes or DAPI-positive total cells (data not shown). The folate level of the medium had no effect on cell numbers, which is consistent with previous studies [34]. These results suggest that neuronal maturation can be affected under low folate conditions at levels that apparently have no effect on cell survival, unlike the complete folate-deficient conditions used in previous studies.

NSPCs differentiate to neurons and glia through strictly regulated processes. Epigenetic mechanisms such as DNA and histone methylation orchestrate neuronal differentiation [2, 3, 4, 5, 6], and loss of DNA methyltransferases, which catalyze DNA methylation, downregulates expression of neural genes and elicits impaired postnatal neurogenesis [35, 36]. H3K4me3 and H3K27me3 also play important roles in transcriptional regulation of several neuronal differentiation-related genes [37, 38]. In this study, murine embryonic telencephalon-derived NSPCs cultured in a low folate medium had decreased methylation of DNA and altered expression of certain neuronal differentiation and maturation-related genes. Low folate-induced changes in gene expression were observed on day 3, when decreased DNA methylation was found under low folate conditions. These results suggest that gene expression changes and epigenetic changes occur in parallel. Significant changes of mRNA expression and DNA methylation were observed for *Neurog1* and *Eomes*. These two genes control neuronal differentiation and are upregulated during neuronal differentiation and downregulated during neuronal maturation in the DG [39, 40, 41]. Tbr2, a transcription factor encoded by *Eomes*, is critically required for progression from NSPCs to neurons in fetal and adult neurogenesis [42, 43]. Tbr2 regulates numerous genes associated with neuronal differentiation and maturation, such as *Neurod1*, which encodes NeuroD1 [44], a basic helix-loop-helix transcription factor that is essential for survival and maturation of newborn neurons and embryonic NSPCs [45, 46, 47] and is downregulated by Tbr2 binding [44]. Despite reduction of DNA methylation and H3K27me3, repressive marks, in the promoter region, the mRNA level for *Neurod1* markedly decreased with low folate in this study. This may be due to strong repression of *Neurod1* transcription by increased Tbr2 binding. Folate deficiency has also been found to affect DNA methylation in neural stem cells under conditions differing from our low folate conditions [48, 49]. These changes in DNA methylation are thought to interfere with normal development of the nervous system. Although the molecular mechanisms of low folate-induced neuronal immaturity cannot be fully explained by changes in only a few genes, DNA hypomethylation in genes associated with neuronal differentiation

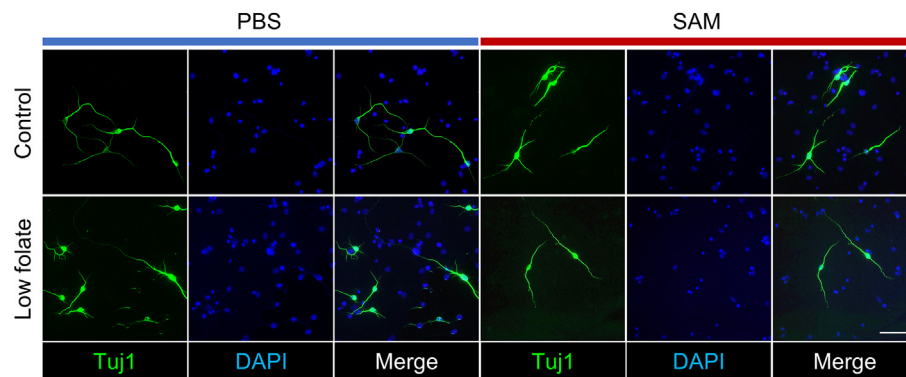
A Day 7 Nestin



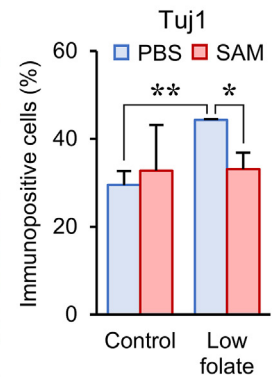
B Day 7



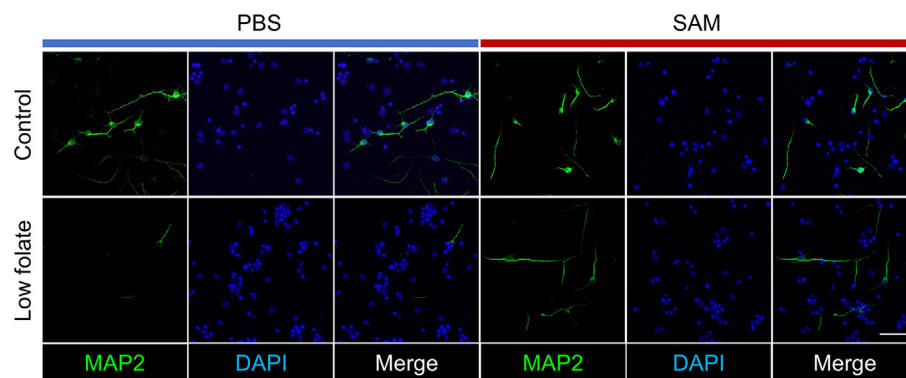
C Day 7 Tuj1



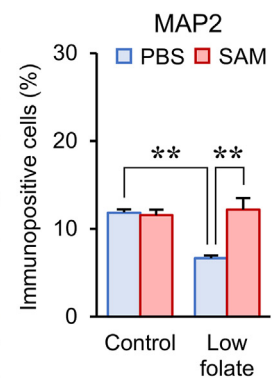
D Day 7



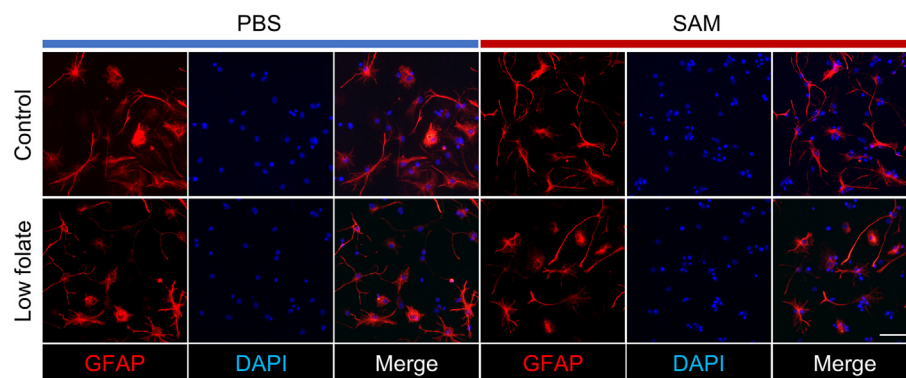
E Day 7 MAP2



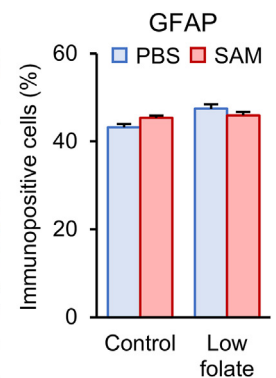
F Day 7



G Day 7 GFAP



H Day 7



(caption on next page)

Figure 6. Effects of SAM supplementation (5 μ M) on abnormalities in neuronal maturation in cells differentiated from NSPCs in a low folate medium on differentiation day 7. Representative photomicrographs of Nestin- (green) (A), Tuj1- (green) (C), MAP2- (green) (E), and GFAP- (red) positive cells (G) were shown. The increased number of Tuj1-positive cells and decreased number of MAP2-positive cells by a low folate medium were reversed by supplementation of SAM. SAM supplementation did not change the numbers of Nestin- or GFAP-positive cells (B,D,F,H). Five visual fields (0.36 mm²) were captured randomly for each well, and data were obtained by averaging the results of the five fields of view. The numbers of the markers-immunopositive cells and DAPI-stained cells were shown in Table 3. The number of cells immunopositive for Nestin, Tuj1, MAP2, or GFAP was determined relative to the number of DAPI-stained nuclei. The percentage of positive cells was determined out of the total number of counted cells stained by DAPI. Values are shown as the mean \pm SEM of 3 cultures. The fold changes were calculated as a ratio to the mean of controls. * $P < 0.05$, ** $P < 0.01$. Scale bar = 30 μ m. Two-way ANOVA revealed a main significant effect of folate ($F_{(1,8)} = 0.85$, $P < 0.05$), but not of SAM ($F_{(1,8)} = 1.60$, $P > 0.05$), and no significant interaction between folate and SAM ($F_{(1,8)} = 0.45$, $P > 0.05$) for Nestin; a main significant effect of folate ($F_{(1,8)} = 9.32$, $P < 0.05$), but not of SAM ($F_{(1,8)} = 0.88$, $P > 0.05$), and no significant interaction between folate and SAM ($F_{(1,8)} = 0.62$, $P > 0.05$) for Tuj1; a main significant effect of folate ($F_{(1,8)} = 8.91$, $P < 0.05$) and SAM ($F_{(1,8)} = 11.90$, $P < 0.01$), and a significant interaction between folate and SAM ($F_{(1,8)} = 14.73$, $P < 0.01$) for MAP2; and no significant effect of folate ($F_{(1,8)} = 2.03$, $P > 0.05$) or SAM ($F_{(1,8)} = 0.78$, $P > 0.05$), and no significant interaction between folate and SAM ($F_{(1,8)} = 0.06$, $P > 0.05$) for GFAP.

and maturation is likely to be involved in this process in a low folate model, as in other models.

In addition to DNA hypomethylation of genes involved in neuronal differentiation and maturation, lower intracellular SAM was observed in cells differentiated in a low folate medium. Furthermore, SAM supplementation reversed low folate-induced expression changes of genes involved in neuronal differentiation and maturation. These results suggest that SAM levels under low folate may be inadequate for dynamic DNA methylation changes in neuronal genes that regulate cellular differentiation and maturation of NSPCs. Reduced intracellular SAM has been shown in complete folate-deficient models [30], and a similar hypomethylation process may occur in a low folate model. Whereas SAM supplementation reversed expression changes of genes involved in neuronal differentiation and maturation, it did not reverse those for genes involved in maintenance and proliferation of NSPCs, such as *Pax6*, *Stat3* and *Hey*. These results suggest that low folate-induced changes in genes involved in maintenance and proliferation of NSPCs may not be caused by lower SAM levels. Immunohistochemistry showed that SAM supplementation improved the neuronal immaturity observed under low folate conditions, which supports the view that low folate-induced abnormalities in neuronal maturation may be due to expression changes of neuronal differentiation and maturation-related genes such as *Neurog1*, *Eomes* and *Neurod1* caused by low SAM.

In conclusion, the current findings suggest that low folate may induce neuronal immaturity via DNA hypomethylation in genes associated with neuronal differentiation and maturation. This DNA hypomethylation may be due to reduction of intracellular SAM levels. These mechanisms may underlie effects in the DG in folate-deficient patients with depression.

Declarations

Author contribution statement

Ryota Araki: Conceived and designed the experiments; Analyzed and interpreted the data; Wrote the paper.

Shoji Nishida: Performed the experiments; Analyzed and interpreted the data; Wrote the paper.

Yuki Nakajima, Arimi Iwakumo, Hayato Tachioka, Ayami Kita: Performed the experiments.

Takeshi Yabe: Conceived and designed the experiments.

Funding statement

This work was supported by JSPS KAKENHI Grant Number JP17K00897, Grant-in-Aid for JSPS Research Fellow Grant Number JP17J03416, and The Food Science Institute Foundation (Ryoushokukenkuyukai).

Data availability statement

Data will be made available on request.

Declaration of interests statement

The authors declare no conflict of interest.

Additional information

No additional information is available for this paper.

Acknowledgements

We thank Keisuke Ota, Ikuyo Harada, Yuko Takenaka, Ryo Takemura, Sota Asari and Shin Tachibana for their technical assistance.

References

- [1] F.H. Gage, Mammalian neural stem cells, *Science* 287 (2000) 1433–1438.
- [2] B. Yao, et al., Epigenetic mechanisms in neurogenesis, *Nat. Rev. Neurosci.* 17 (2016) 537–549.
- [3] K.D. Rhee, J. Yu, C.Y. Zhao, G. Fan, X.J. Yang, Dnmt1-dependent DNA methylation is essential for photoreceptor terminal differentiation and retinal neuron survival, *Cell Death Dis.* 3 (2012) e427.
- [4] H. Wu, et al., Dnmt3a-dependent nonpromoter DNA methylation facilitates transcription of neurogenic genes, *Science* 329 (2010) 444–448.
- [5] H. Noguchi, et al., Expression of DNMT1 in neural stem/precursor cells is critical for survival of newly generated neurons in the adult hippocampus, *Neurosci. Res.* 95 (2015) 1–11.
- [6] J. Feng, et al., Dnmt1 and Dnmt3a maintain DNA methylation and regulate synaptic function in adult forebrain neurons, *Nat. Neurosci.* 13 (2010) 423–430.
- [7] A.M. Bond, G.L. Ming, H. Song, Adult mammalian neural stem cells and neurogenesis: five decades later, *Cell Stem Cell* 17 (2015) 385–395.
- [8] J.S. Snyder, A. Soumier, M. Brewer, J. Pickel, H.A. Cameron, Adult hippocampal neurogenesis buffers stress responses and depressive behaviour, *Nature* 476 (2011) 458–461.
- [9] L. Santarelli, et al., Requirement of hippocampal neurogenesis for the behavioral effects of antidepressants, *Science* 301 (2003) 805–809.
- [10] T.J. Schoenfeld, H.A. Cameron, Adult neurogenesis and mental illness, *Neuropsychopharmacology* 40 (2015) 113–128.
- [11] O.S. Anderson, K.E. Sant, D.C. Dolinoy, Nutrition and epigenetics: an interplay of dietary methyl donors, one-carbon metabolism and DNA methylation, *J. Nutr. Biochem.* 23 (2012) 853–859.
- [12] A. Desai, J.M. Sequeira, E.V. Quadros, The metabolic basis for developmental disorders due to defective folate transport, *Biochimie* 126 (2016) 31–42.
- [13] A.E. Czeizel, I. Dudas, A. Vereczkey, F. Banhidy, Folate deficiency and folic acid supplementation: the prevention of neural-tube defects and congenital heart defects, *Nutrients* 5 (2013) 4760–4775.
- [14] M.W. Carney, et al., Red cell folate concentrations in psychiatric patients, *J. Affect. Disord.* 19 (1990) 207–213.
- [15] M.W. Carney, B.F. Sheffield, Serum folic acid and B12 in 272 psychiatric inpatients, *Psychol. Med.* 8 (1978) 139–144.
- [16] A.M. Ghadirian, J. Ananth, F. Engelsmann, Folic acid deficiency and depression, *Psychosomatics* 21 (1980) 926–929.
- [17] E.H. Reynolds, J.M. Preece, J. Bailey, A. Coppen, Folate deficiency in depressive illness, *Br. J. Psychiatry* : *J. Ment. Sci.* 117 (1970) 287–292.
- [18] D.W. Morris, M.H. Trivedi, A.J. Rush, Folate and unipolar depression, *J. Alternative Compl. Med.* 14 (2008) 277–285.
- [19] S. Gilbody, T. Lightfoot, T. Sheldon, Is low folate a risk factor for depression? A meta-analysis and exploration of heterogeneity, *J. Epidemiol. Community Health* 61 (2007) 631–637.
- [20] A. Bender, K.E. Hagan, N. Kingston, The association of folate and depression: a meta-analysis, *J. Psychiatr. Res.* 95 (2017) 9–18.
- [21] S. Nishida, et al., Post-weaning folate deficiency induces a depression-like state via neuronal immaturity of the dentate gyrus in mice, *J. Pharmacol. Sci.* (2020).
- [22] T. Yabe, et al., Ferulic acid induces neural progenitor cell proliferation in vitro and in vivo, *Neuroscience* 165 (2010) 515–524.

- [23] G. Rumbaugh, C.A. Miller, Epigenetic changes in the brain: measuring global histone modifications, *Methods Mol. Biol.* 670 (2011) 263–274.
- [24] R. Araki, et al., Epigenetic regulation of dorsal raphe GABA associated with isolation-induced abnormal responses to social stimulation in mice, *Neuropharmacology* 101 (2015) 1–12.
- [25] D. Takai, P.A. Jones, Comprehensive analysis of CpG islands in human chromosomes 21 and 22, *Proc. Natl. Acad. Sci. U. S. A.* 99 (2002) 3740–3745.
- [26] M. Gardiner-Garden, M. Frommer, CpG islands in vertebrate genomes, *J. Mol. Biol.* 196 (1987) 261–282.
- [27] B. Schuettengruber, A.M. Martinez, N. Iovino, G. Cavalli, Trithorax group proteins: switching genes on and keeping them active, *Nat. Rev. Mol. Cell Biol.* 12 (2011) 799–814.
- [28] K.S. Crider, T.P. Yang, R.J. Berry, L.B. Bailey, Folate and DNA methylation: a review of molecular mechanisms and the evidence for folate's role, *Adv Nutr* 3 (2012) 21–38.
- [29] Kruman II, P.R. Mouton, R. Emokpae Jr., R.G. Cutler, M.P. Mattson, Folate deficiency inhibits proliferation of adult hippocampal progenitors, *Neuroreport* 16 (2005) 1055–1059.
- [30] N. Akchiche, et al., Homocysteinylation of neuronal proteins contributes to folate deficiency-associated alterations of differentiation, vesicular transport, and plasticity in hippocampal neuronal cells, *Faseb. J.* 26 (2012) 3980–3992.
- [31] R. Kerek, et al., Early methyl donor deficiency may induce persistent brain defects by reducing Stat3 signaling targeted by miR-124, *Cell Death Dis.* 4 (2013) e755.
- [32] A. Geoffroy, et al., Developmental impairments in a rat model of methyl donor deficiency: effects of a late maternal supplementation with folic acid, *Int. J. Mol. Sci.* 20 (2019).
- [33] A. Geoffroy, et al., Late maternal folate supplementation rescues from methyl donor deficiency-associated brain defects by restoring let-7 and miR-34 pathways, *Mol. Neurobiol.* 54 (2017) 5017–5033.
- [34] Y. Chen, et al., Folic acid deficiency inhibits neural rosette formation and neuronal differentiation from rhesus monkey embryonic stem cells, *J. Neurosci. Res.* 90 (2012) 1382–1391.
- [35] S. Nguyen, K. Meletis, D. Fu, S. Jhaveri, R. Jaenisch, Ablation of de novo DNA methyltransferase Dnmt3a in the nervous system leads to neuromuscular defects and shortened lifespan, *Dev. Dynam.* 236 (2007) 1663–1676.
- [36] G. Fan, et al., DNA methylation controls the timing of astrogliogenesis through regulation of JAK-STAT signaling, *Development* 132 (2005) 3345–3356.
- [37] J.D. Pereira, et al., Ezh2, the histone methyltransferase of PRC2, regulates the balance between self-renewal and differentiation in the cerebral cortex, *Proc. Natl. Acad. Sci. U. S. A.* 107 (2010) 15957–15962.
- [38] D.A. Lim, et al., Chromatin remodelling factor Mll1 is essential for neurogenesis from postnatal neural stem cells, *Nature* 458 (2009) 529–533.
- [39] R.D. Hodge, et al., Intermediate progenitors in adult hippocampal neurogenesis: Tbr2 expression and coordinate regulation of neuronal output, *J. Neurosci. : Off. J. Soci. Neurosci.* 28 (2008) 3707–3717.
- [40] C. Schuurmans, et al., Sequential phases of cortical specification involve Neurogenin-dependent and -independent pathways, *EMBO J.* 23 (2004) 2892–2902.
- [41] E.J. Kim, et al., Spatiotemporal fate map of neurogenin1 (Neurog1) lineages in the mouse central nervous system, *J. Comp. Neurol.* 519 (2011) 1355–1370.
- [42] R.D. Hodge, et al., Tbr2 is essential for hippocampal lineage progression from neural stem cells to intermediate progenitors and neurons, *J. Neurosci. : Off. J. Soci. Neurosci.* 32 (2012) 6275–6287.
- [43] A.B. Mihalas, et al., Intermediate progenitor cohorts differentially generate cortical layers and require Tbr2 for timely acquisition of neuronal subtype identity, *Cell Rep.* 16 (2016) 92–105.
- [44] A. Sessa, et al., The Tbr2 molecular network controls cortical neuronal differentiation through complementary genetic and epigenetic pathways, *Cerebr. Cortex* 27 (2017) 5715.
- [45] Z. Gao, et al., Neurod1 is essential for the survival and maturation of adult-born neurons, *Nat. Neurosci.* 12 (2009) 1090–1092.
- [46] A. Pataskar, et al., NeuroD1 reprograms chromatin and transcription factor landscapes to induce the neuronal program, *EMBO J.* 35 (2016) 24–45.
- [47] C. Boutin, et al., NeuroD1 induces terminal neuronal differentiation in olfactory neurogenesis, *Proc. Natl. Acad. Sci. U. S. A.* 107 (2010) 1201–1206.
- [48] X. Wang, et al., Genomic DNA hypomethylation is associated with neural tube defects induced by methotrexate inhibition of folate metabolism, *PLoS One* 10 (2015), e0121869.
- [49] S. Luo, et al., Folic acid acts through DNA methyltransferases to induce the differentiation of neural stem cells into neurons, *Cell Biochem. Biophys.* 66 (2013) 559–566.